Nuclear Structure Theory (lecture III)

Gianluca Colò
Dep. of Physics and
INFN, Milano

“Collective” spectroscopy

Nuclear spectroscopy

In Magda's lectures: ample discussions about the **relationships between observable properties of the low-lying spectra and nuclear shapes**.

In lecture II we have also introduced the paradigmatic case of vibrational and rotational nuclei.

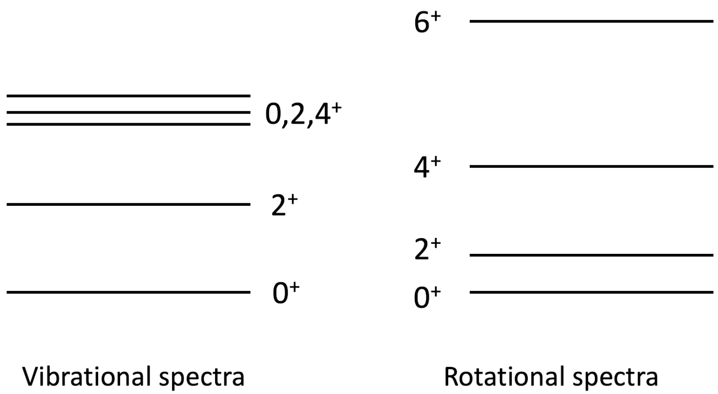

Can DFT handle the case of shape coexistence?

Transition between spherical and well-deformed nuclei

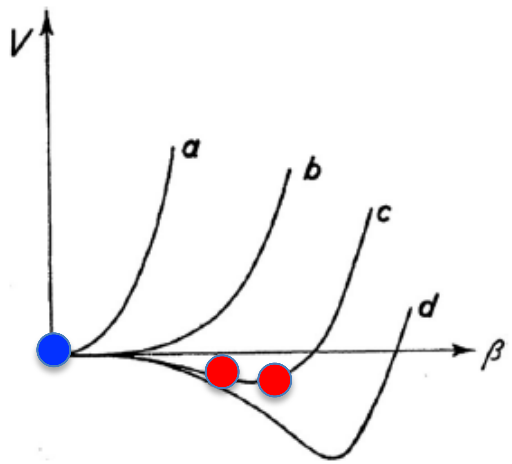

When the potential is not very stiff, it is quite natural to assume that the **density is not the one corresponding to a single value of β or < Q >**.

The density can be seen as a superposition of the densities associated with different quadrupole deformations β.

$$|\Psi\rangle = \int dq\ f(q)|\Phi(q)\rangle \qquad E = \frac{\langle\Psi|H|\Psi\rangle}{\langle\Psi|\Psi\rangle}$$

- The energy should be minimized (again, variational principle).
- Generator coordinate method or **multi-reference DFT**.
- Angular momentum projection needed!

Examples of multi-reference DFT calculations

Values of the total energy

J. Xiang *et al.*
PRC 93, 054324 (2016)

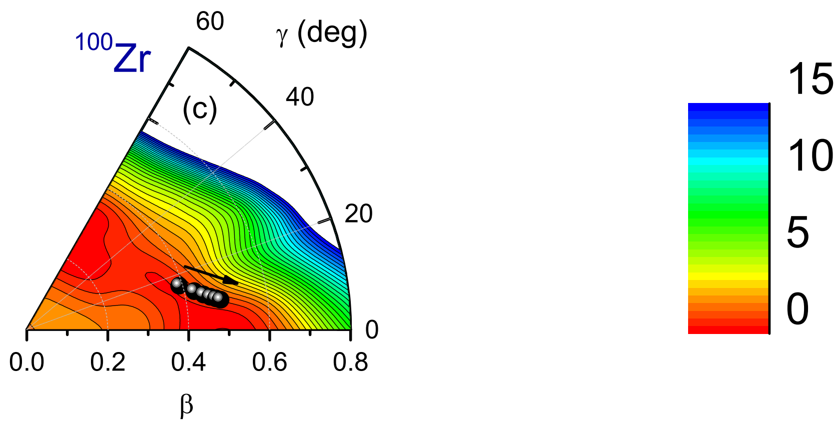

Systematic calculations of the low-lying states

Y.L. Yang *et al.* PRC 197, 024308 (2023)

$$B(E\lambda, i \to f) = \frac{1}{2J_i + 1} \langle f || O_{\lambda\mu,EL} || i \rangle^2$$

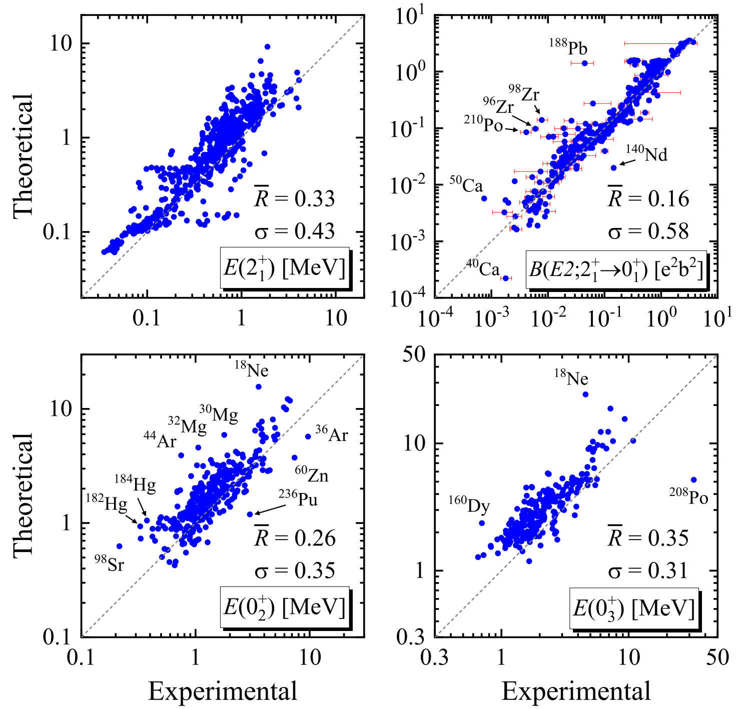

Changing the quadrupole moment or?

The shapes of nuclei

G.F. Bertsch*

Department of Physics and Institute for Nuclear Theory,

University of Washington, Seattle, Washington 98915, USA

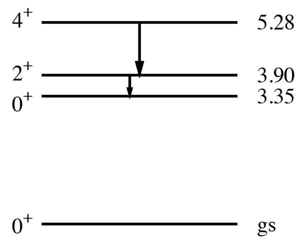

FIG. 3: The spectrum of ^{40}Ca, showing the first three levels of the deformed band and the gamma transitions that establish the deformation of the band [11]

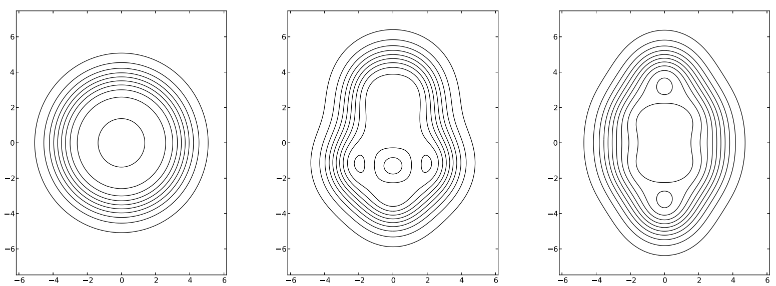

FIG. 5: Density distribution of the ^{40}Ca configurations. Left: ground state; center: GCM configuration at $q = 108$ fm^2; right: 4p-4h K^π-constrained configuration.

Instead of Q **one can put a constraint on the number of particles that are promoted to the next shell.**

Nuclear spectra above the particle threshold

At “high” energy, above the particle emission threshold, there is a continuum of states – and yet some prominent states show up: **the Giant Resonances.**

They lie around 10-30 MeV, and they have large widths.

$$\tau = \frac{\hbar}{\Gamma}$$

They can undergo particle emission.

They are “giant” because they have large cross sections.

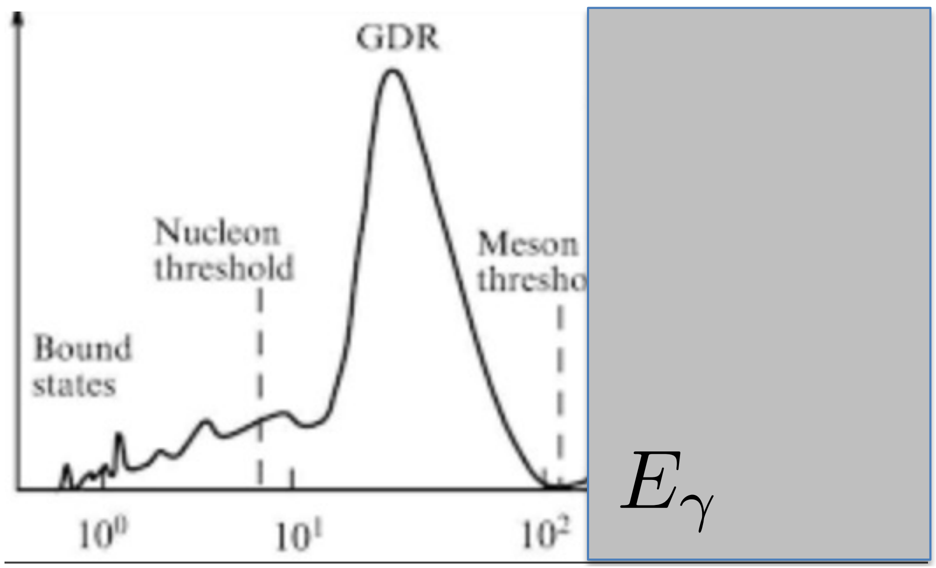

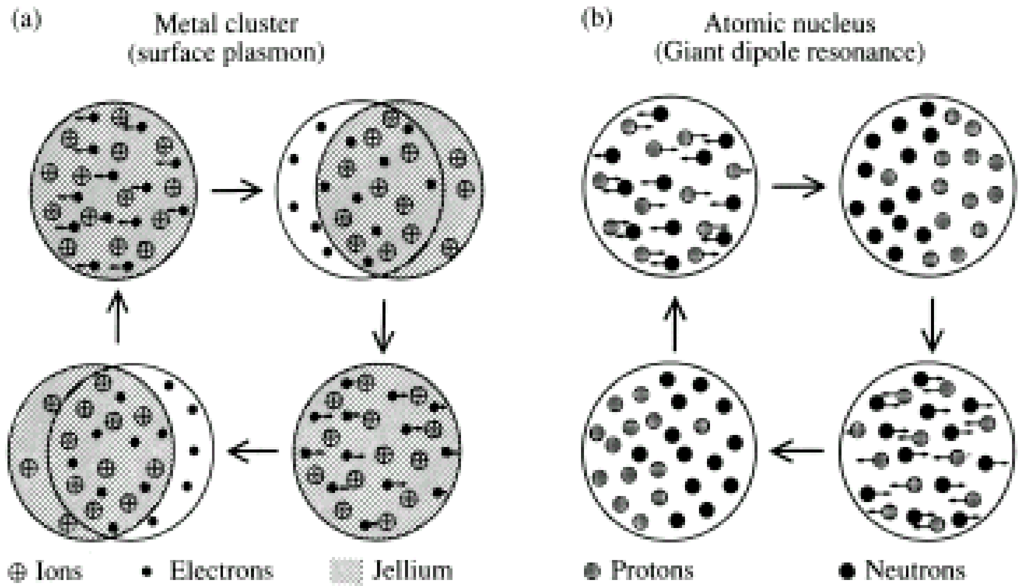

Dipole oscillations: isovector

- GDR (Giant Dipole Resonance): excited by a photon beam impinging on a nucleus.

$$\hbar c \approx 197 \text{ MeV fm}$$

- E ≈ 10-20 MeV implies that $\lambda_{el.field} = hc / E >> R$ (nuclear dimension).
- Consequently, **the e.m. field in the nuclear region can be considered constant (dipole approximation)**.

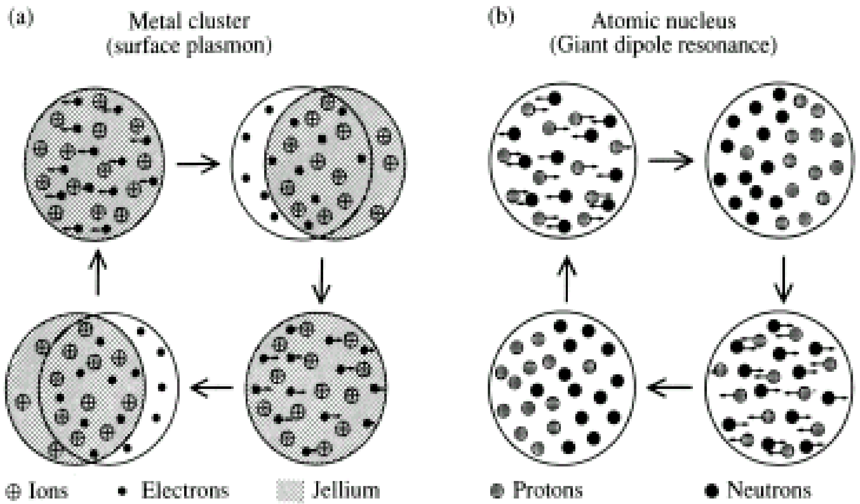

- Analogy with excitations in molecules or solids (plasmons)
- In nuclei there have been intensive searches of “pygmy” dipole states.

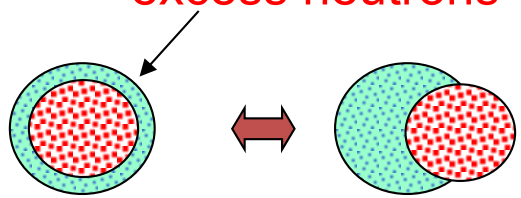

"Pygmy" dipole resonance (?)

Progress in Particle and Nuclear Physics 70 (2013) 210–245

Contents lists available at SciVerse ScienceDirect

Progress in Particle and Nuclear Physics

journal homepage: www.elsevier.com/locate/ppnp

ELSEVIER

Review

Experimental studies of the Pygmy Dipole Resonance

D. Savran [a,b,*], T. Aumann [c,d], A. Zilges [e]

Progress in Particle and Nuclear Physics 129 (2023) 104006

Contents lists available at ScienceDirect

Progress in Particle and Nuclear Physics

journal homepage: www.elsevier.com/locate/ppnp

ELSEVIER

Review

Theoretical studies of Pygmy Resonances

E.G. Lanza [a,b,*], L. Pellegri [c,d], A. Vitturi [e,f], M.V. Andrés [g]

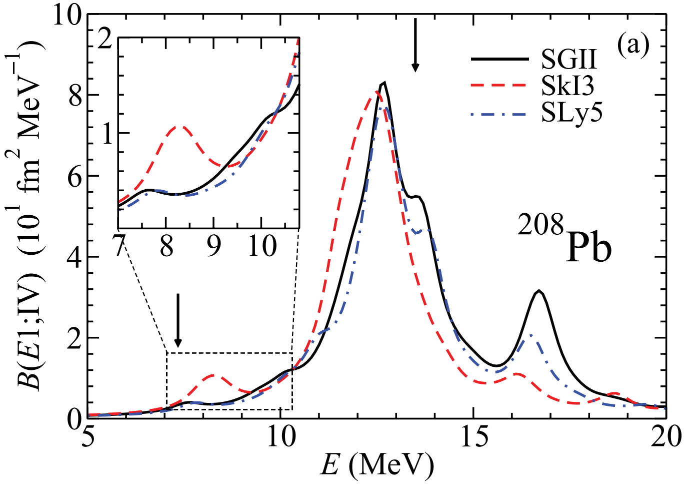

There have been strong discussions if it really exists.

"Resonance" or SPS?

Impact for (n,γ): cf. Ann-Cecile.

Vortex photons

Use of photons with orbital angular momentum can open new avenues for the physics of collective states.

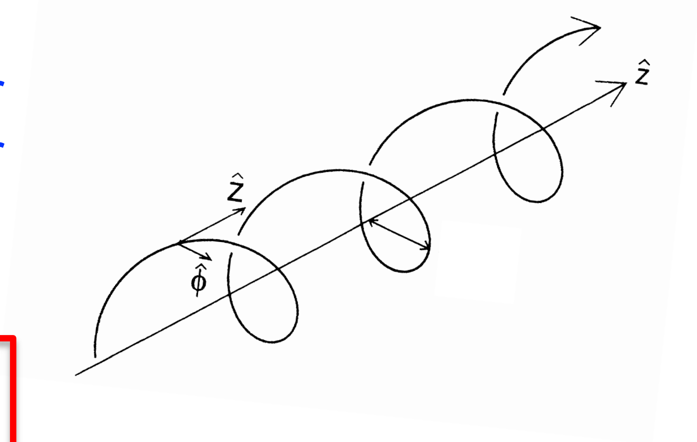

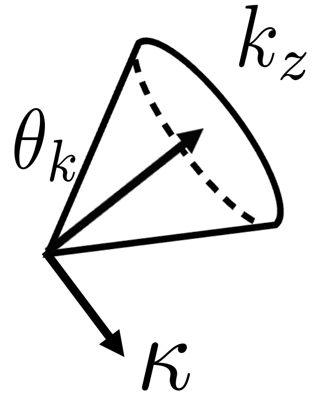

$$M_f - M_i = m_\gamma = m_\ell + m_s$$

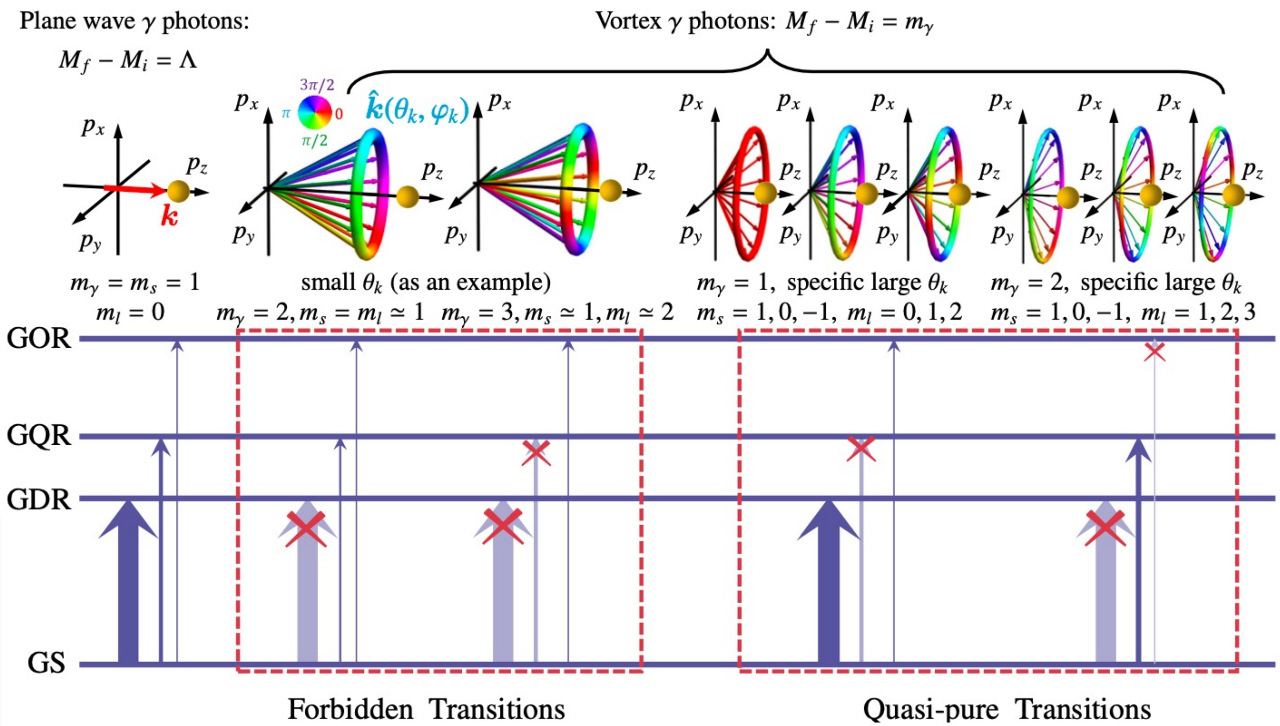

Z.W. Lu *et al.*, Phys. Rev. Lett. 131, 202502 (2023)

Types of giant resonances

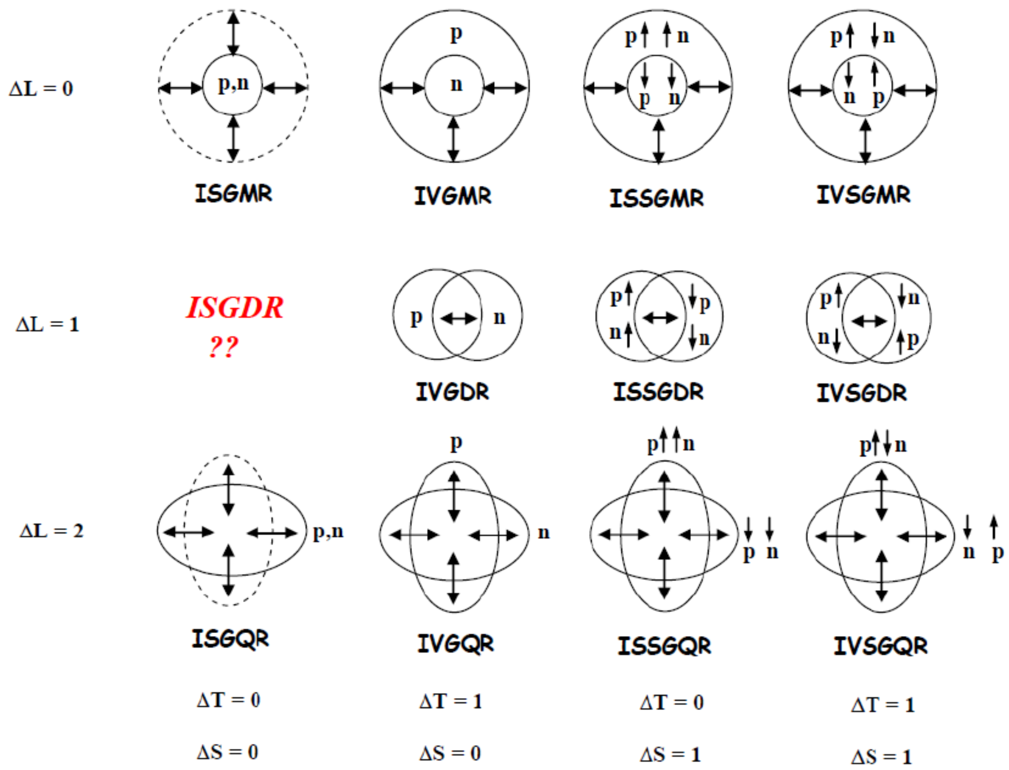

Image courtesy of M. Harakeh

IS = Iso-Scalar
IV = Iso-Vector
S = Spin
G = Giant
M = Monopole
D = Dipole
Q = Quadrupole
O = Octupole

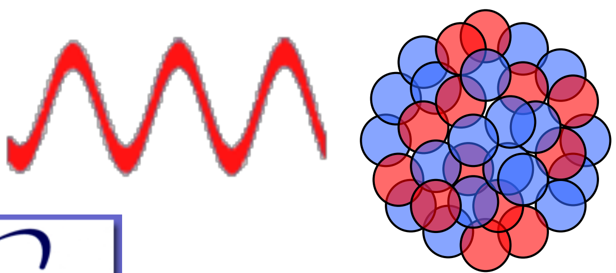

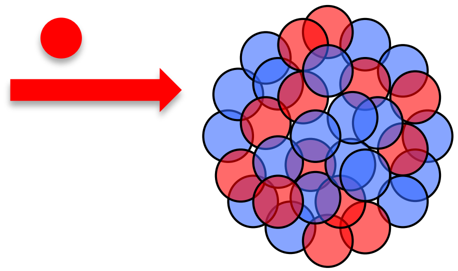

They are excited by photons or by particle inelastic scattering

Strength function and operators

$$S(E) = \sum_n |\langle n|F|0\rangle|^2 \, \delta\left(E - E_n\right)$$

$$S(E) = \sum_n |\langle n|F|0\rangle|^2 \frac{\Gamma_n}{\left(E - E_n\right)^2 + \frac{\Gamma_n^2}{4}}$$

$$F_{\mathrm{IS}} = \sum_i r_i^L Y_{LM}(\hat{r}_i),$$

$$F_{\mathrm{IV}} = \sum_i r_i^L Y_{LM}(\hat{r}_i)\tau_z(i).$$

$$F_{\mathrm{IS}} = \sum_i r_i^L \left[Y_{LM}(\hat{r}_i) \otimes \boldsymbol{\sigma}(i)\right]_J,$$

$$F_{\mathrm{IV}} = \sum_i r_i^L \left[Y_{LM}(\hat{r}_i) \otimes \boldsymbol{\sigma}(i)\right]_J \tau_z(i).$$

$$F_{\mathrm{ISGMR}} = \sum_i r_i^2,$$

$$F_{\mathrm{IVGMR}} = \sum_i r_i^2 \tau_z(i).$$

$$F_{\mathrm{IVGDR}} = \frac{eN}{A}\sum_{i=1}^{Z} r_i Y_{1M}(\hat{r}_i) - \frac{eZ}{A}\sum_{i=1}^{N} r_i Y_{1M}(\hat{r}_i).$$

The Giant Monopole Resonance

Breathing mode: in this case its energy is correlated with the compressibility of nuclear matter.

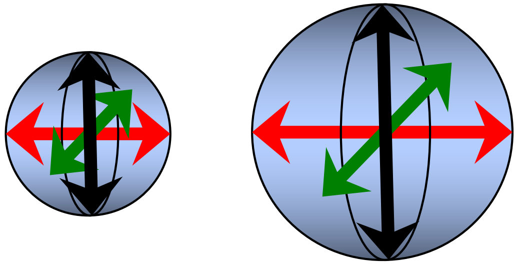

$$\chi \equiv -\frac{1}{\Omega}\left(\frac{\partial P}{\partial \Omega}\right)^{-1}$$

$$K_\infty = 9\rho_0^2 \frac{d^2}{d\rho^2}\left(\frac{E}{A}\right)_{\rho=\rho_0}$$

We better consider the density as a variable. $\rho = \frac{A}{\Omega}$ Incompressibility: $\chi^{-1} = \rho^3 \frac{d^2}{d\rho^2}\left(\frac{E}{A}\right)$

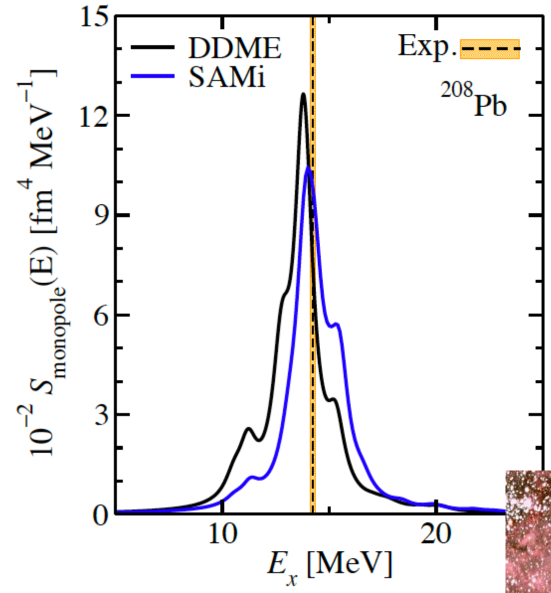

PHYSICAL REVIEW LETTERS **129,** 032701 (2022)

Probing the Incompressibility of Nuclear Matter at Ultrahigh Density through the Prompt Collapse of Asymmetric Neutron Star Binaries

Albino Perego,[1,2,*] Domenico Logoteta,[3,4] David Radice,[5,6,7] Sebastiano Bernuzzi,[8] Rahul Kashyap,[5,6] Abhishek Das,[5,6] Surendra Padamata,[5,6] and Aviral Prakash[5,6]

U. Garg, GC, PPNP 101 (2018) 55

Charge-exchange transitions and β-decay

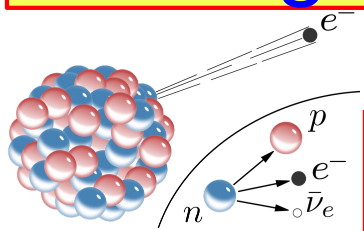

They are induced by reactions, like (p,n) or (^{3}He,t).

Some transitions may be inside the allowed β-decay window.

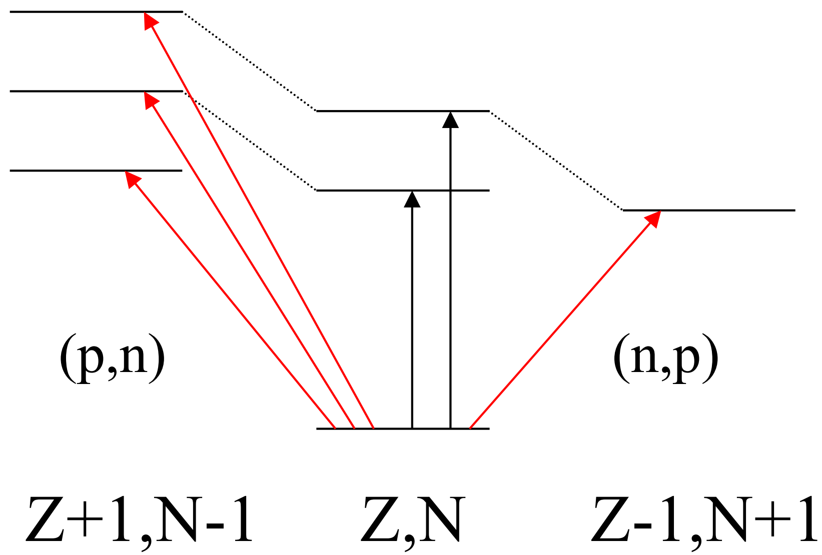

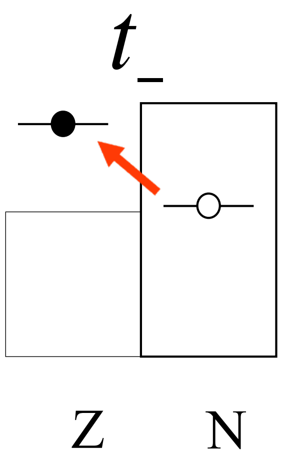

$$j_< = \ell - \frac{1}{2}$$

$$j_> = \ell + \frac{1}{2}$$

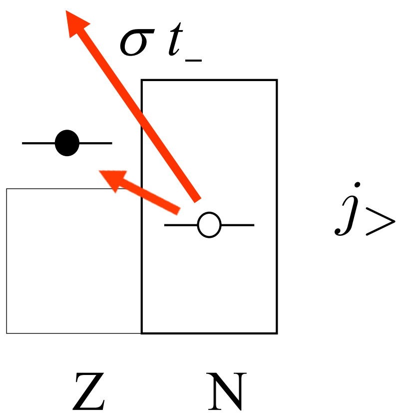

Isobaric Analog State:
n changed into p

Gamow-Teller Resonance:
also spin-flip

Giant Resonances and highly excited states
Spectroscopy of heavy and superheavy nuclei
Reactions (transfer, fusion, fission)
Neutron stars

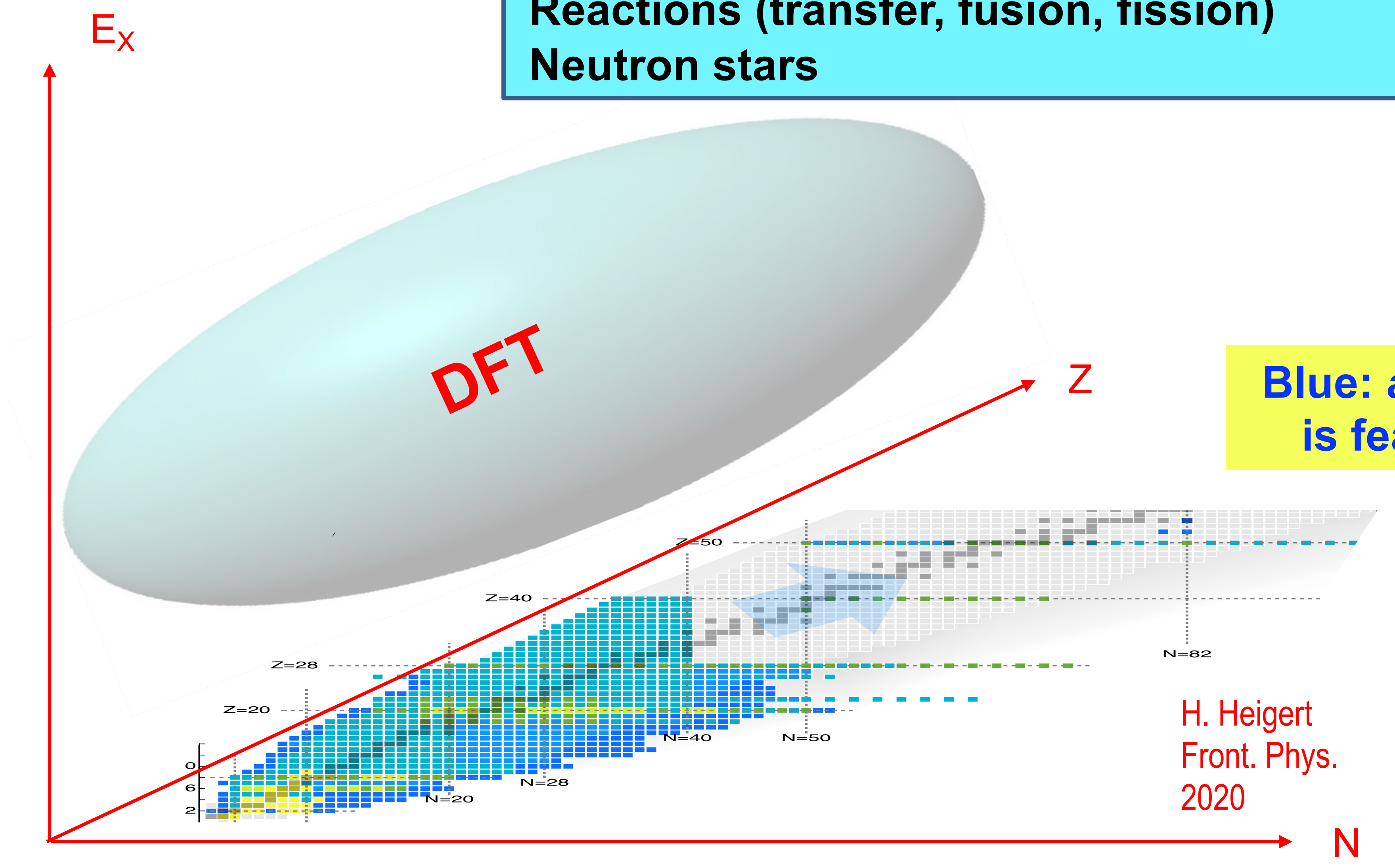

Blue: *ab initio* is feasible

H. Heigert
Front. Phys.
2020

Time-dependent DFT and RPA

$$h\phi_i = \varepsilon_i \phi_i$$

From: P. Stevenson (U. Surrey)

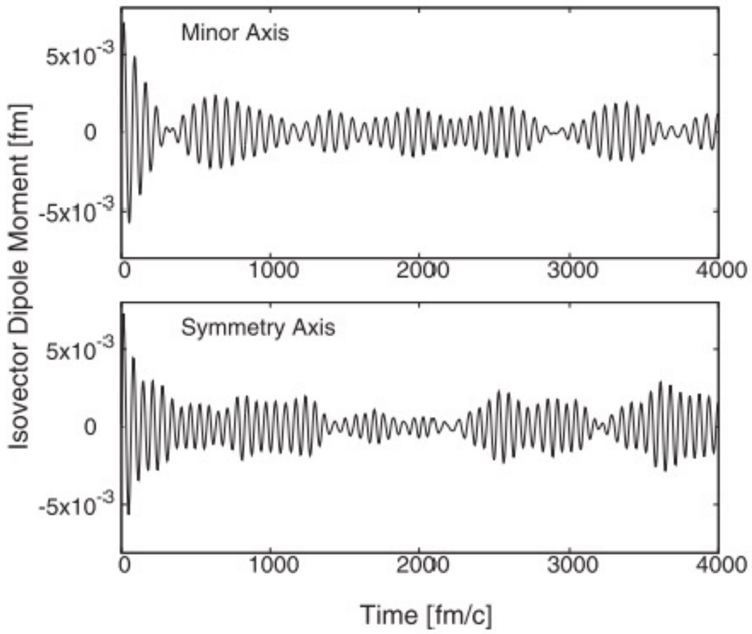

In the time-dependent case, one can solve the evolution equation for the density directly:

$$h(t) = h + f(t) \qquad [h(t), \rho(t)] = i\hbar\, \dot{\rho}(t)$$

$$\rho(t=0) \neq \rho_{\mathrm{g.s.}}$$

$$\rho(t=\Delta t) = U(t=0, t=\Delta t)\rho(t=0) \qquad U = e^{-i\frac{\Delta t}{\hbar}\cdot h}$$

If the equation for the density is **linearized** and solved on a basis: **Random Phase Approximation or RPA.**

$$\begin{pmatrix} A & B \\ -B^* & -A^* \end{pmatrix} \begin{pmatrix} X \\ Y \end{pmatrix} = \hbar\omega \begin{pmatrix} X \\ Y \end{pmatrix}$$

G.C. *et al.*, Computer Physics Commun. 184, 142 (2013).

In RPA the excited states are 1p-1h superpositions

The external field excites, at lowest order, a one particle-one hole state (1p-1h)

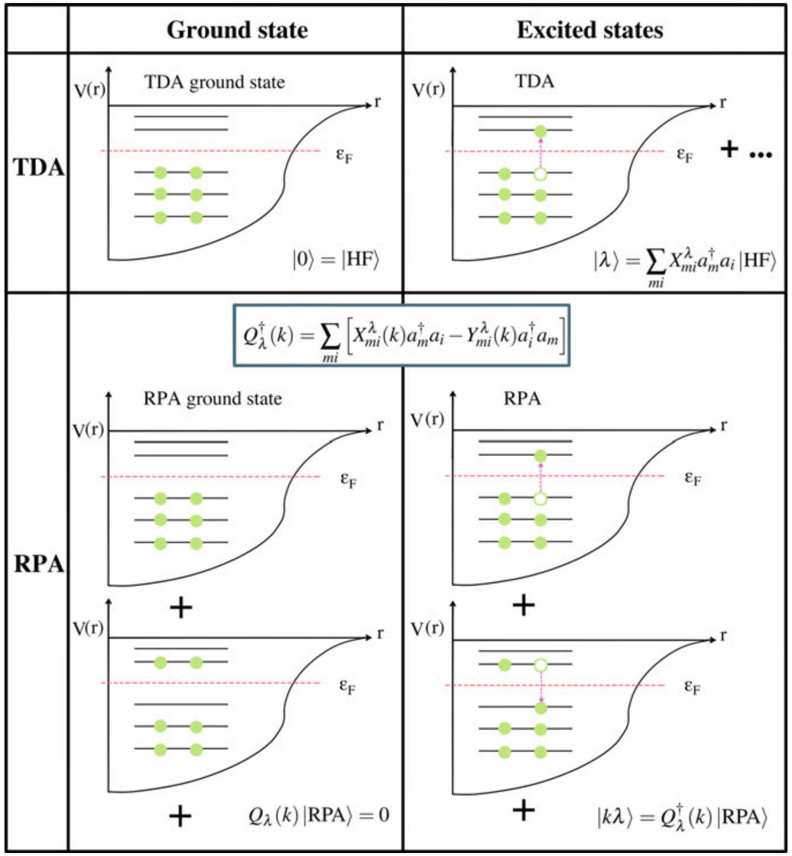

Figure taken from: A. Obertelli and H. Sagawa, *Modern Nuclear Physics*, Springer (2021)

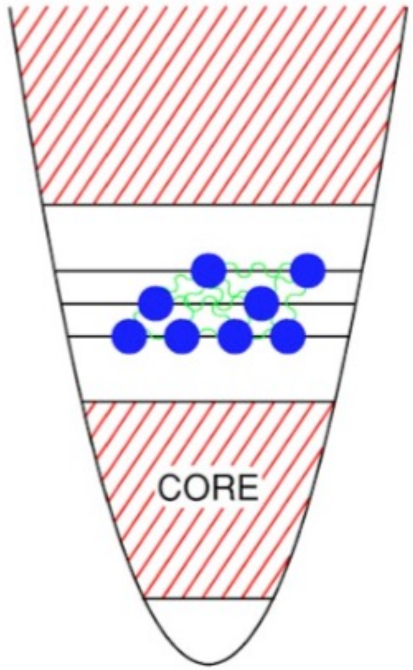

One can extend RPA to second RPA (2p-2h)
Advantage of Shell Model: automatically, many p-many h included.
Advantage of RPA: possibility to go to large model spaces (in other terms, "no core".

Random Phase Approximation (RPA)

$$\begin{pmatrix} \varepsilon_{\rm ph} + v_{\rm ph,ph} & v_{\rm ph,p'h'} & \cdots \\ v_{\rm p'h',ph} & \varepsilon_{\rm p'h'} + v_{\rm p'h',p'h'} & \cdots \\ \cdots & \cdots & \cdots \end{pmatrix}$$

In RPA (or TDA) the excited states are **superpositions of particle-hole excitations**, that interfere to form a state that we can view as an excitation of the nucleus as a whole. Cf. the picture below and the toy model in the next slides.

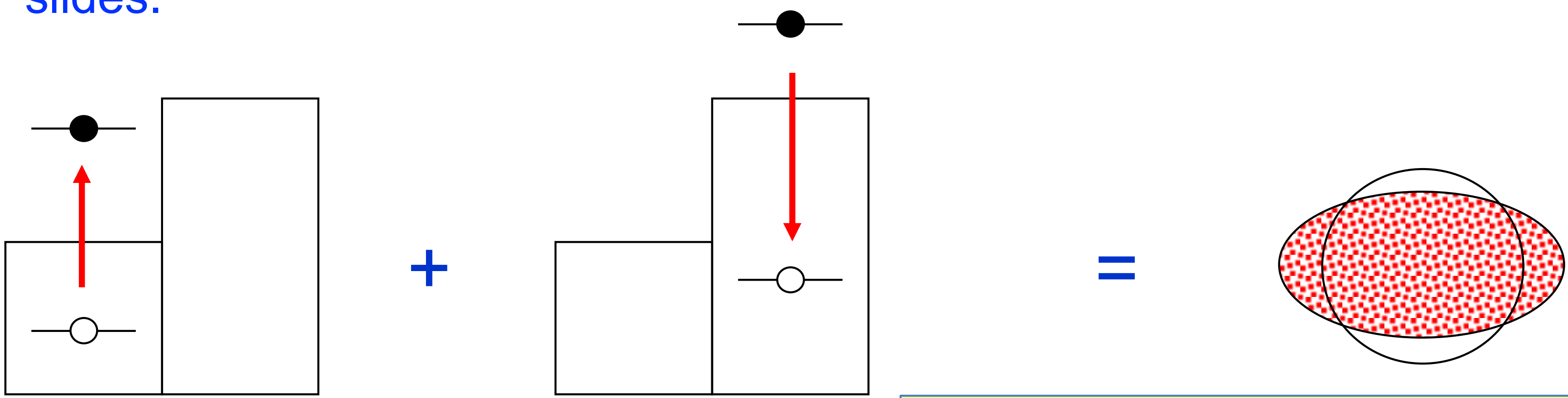

$$|n\rangle = \left(\sum_{ph} X^{(n)}_{\rm ph} a^\dagger_p a_h - Y^{(n)}_{\rm ph} a^\dagger_h a_p \right) |\tilde{0}\rangle$$

PHYSICAL REVIEW LETTERS **121,** 252501 (2018)

Enhanced Quadrupole and Octupole Strength in Doubly Magic ^{132}Sn

D. Rosiak,[1] M. Seidlitz,[1,*] P. Reiter,[1] H. Naïdja,[2,3,4] Y. Tsunoda,[5] T. Togashi,[5] F. Nowacki,[2,3] T. Otsuka,[6,5,7,8,9] G. Colò,[10,11] K. Arnswald,[1] T. Berry,[12] A. Blazhev,[1] M. J. G. Borge,[13,†] J. Cederkäll,[14] D. M. Cox,[15,16] H. De Witte,[8] L. P. Gaffney,[13] C. Henrich,[17] R. Hirsch,[1] M. Huyse,[8] A. Illana,[8] K. Johnston,[13] L. Kaya,[1] Th. Kröll,[17] M. L. Lozano Benito,[13] J. Ojala,[15,16] J. Pakarinen,[15,16] M. Queiser,[1] G. Rainovski,[18] J. A. Rodriguez,[13] B. Siebeck,[1] E. Siesling,[13] J. Snäll,[14] P. Van Duppen,[8] A. Vogt,[1] M. von Schmid,[17] N. Warr,[1] F. Wenander,[13] and K. O. Zell[1]

(MINIBALL and HIE-ISOLDE Collaborations)

theory [11,12]. Because of the computational limits of the valence space, the SM approaches do not provide information on the 3_1^- state. The RPA and RRPA calculations

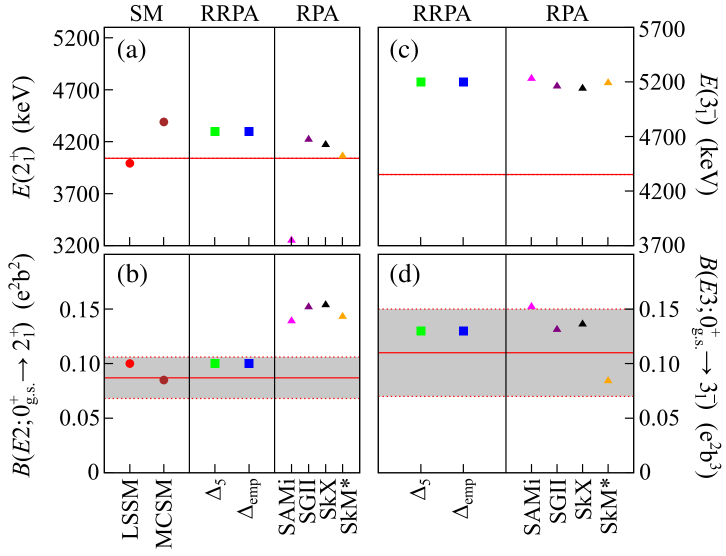

Exercise(s): try yourself comparison between RPA and SM.

ns4exp.mi.infn.it

Limitations: RPA only for spherical systems, SM not suitable for large model spaces.

RPA and collectivity: schematic model (I)

Schematic 2 x 2 case

$$\begin{pmatrix} \varepsilon + v & v \\ v & \varepsilon + v \end{pmatrix}$$

$$\hbar\omega_1 = \varepsilon, \qquad X^{(1)} = \frac{1}{\sqrt{2}} \begin{pmatrix} 1 \\ -1 \end{pmatrix},$$

$$\hbar\omega_2 = \varepsilon + v \qquad X^{(2)} = \frac{1}{\sqrt{2}} \begin{pmatrix} 1 \\ 1 \end{pmatrix}.$$

Magnetic spin-flip states (M1)

^{208}Pb : $h_{11/2} \rightarrow h_{9/2}$ (proton)
$i_{13/2} \rightarrow i_{11/2}$ (neutron)

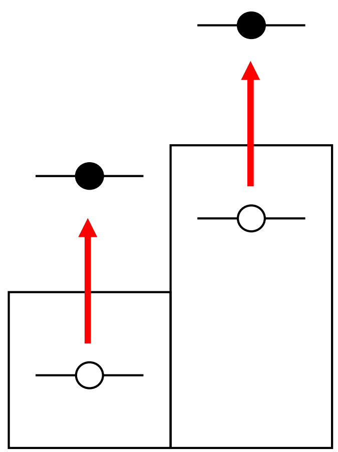

RPA and collectivity: schematic model (II)

Schematic *N* x *N* case

There is one "coherent state":

$$\frac{1}{\sqrt{N}}\begin{pmatrix} 1 \\ 1 \\ \cdots \\ 1 \end{pmatrix}$$

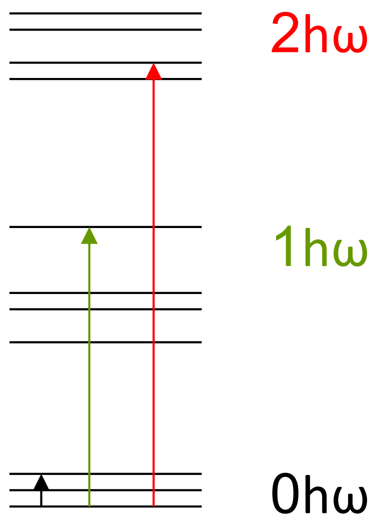

Its transition amplitude is enhanced:

$$\langle n|F|0\rangle = \sum_{ph} X_{ph}\langle p|F|h\rangle \approx N\frac{1}{\sqrt{N}}M = \sqrt{N}\ M$$

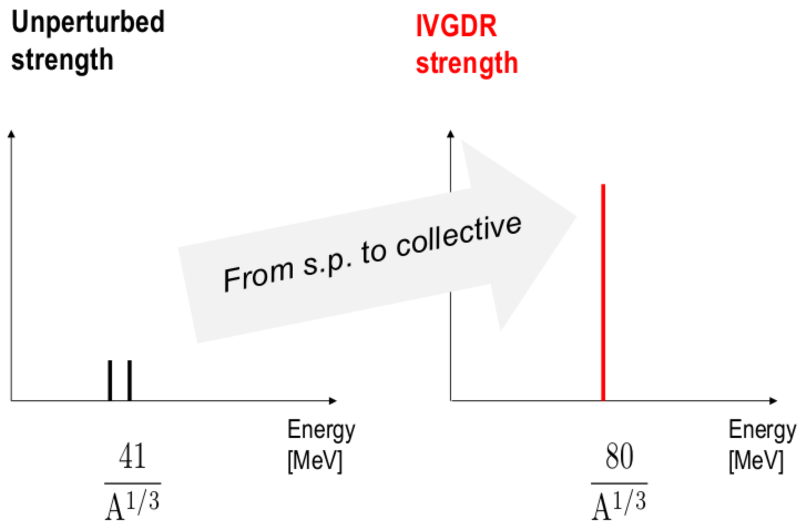

G. C., *Theoretical Methods for Giant Resonances*, in: Handbook of Nuclear Physics, edited by I. Tanihata, H. Toki and T. Kajino (Springer, 2022).

Single-particle spectroscopy

Single-particle spectroscopy: neutron-rich and neutron-deficient nuclei

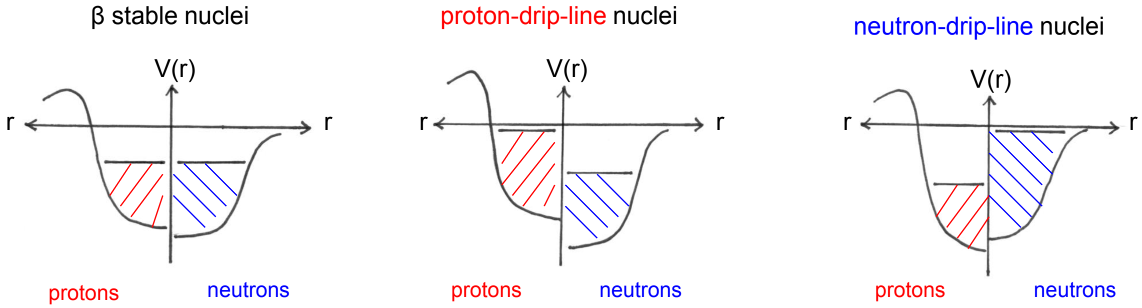

If the neutron number increases, neutrons occupies higher levels – protons become more bound due to the dominance of the p-n interaction.

I. Hamamoto and H. Sagawa, Phys. Rev. C48, R960 (1993)

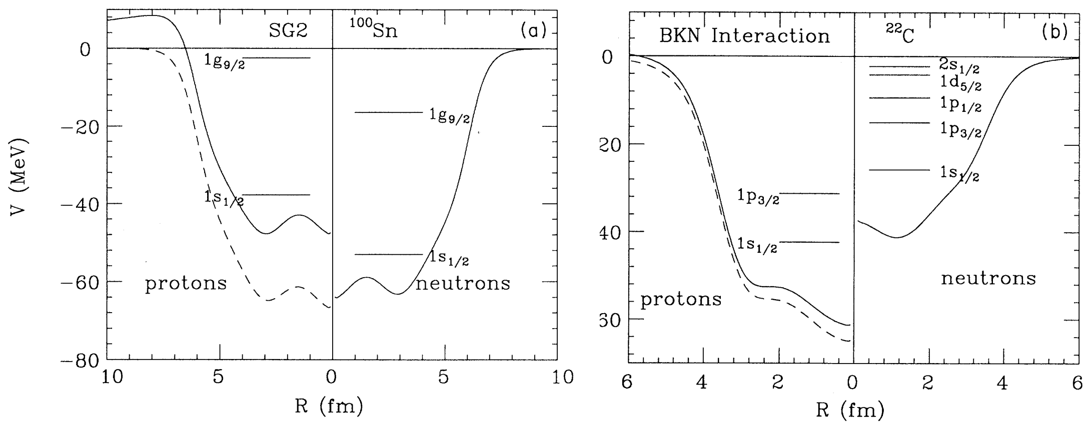

I. Talmi and I. Unna, Phys. Rev. Lett. 4, 469 (1960)

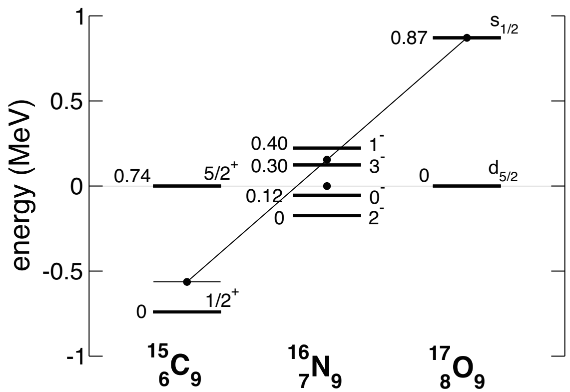

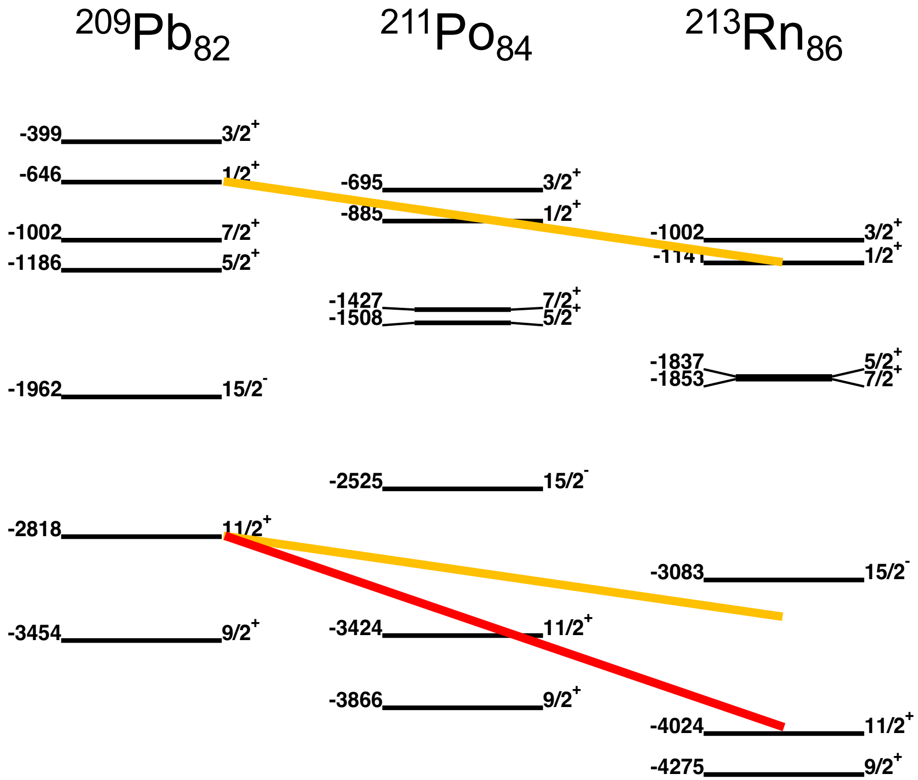

Changes of orbitals (either upward or downward) are LARGER for HIGHER angular momenta.

In fact, orbitals with <u>smaller values of angular momenta are less constrained by the centrifugal barrier and overlap less with the other states.</u>

(pf-shell)

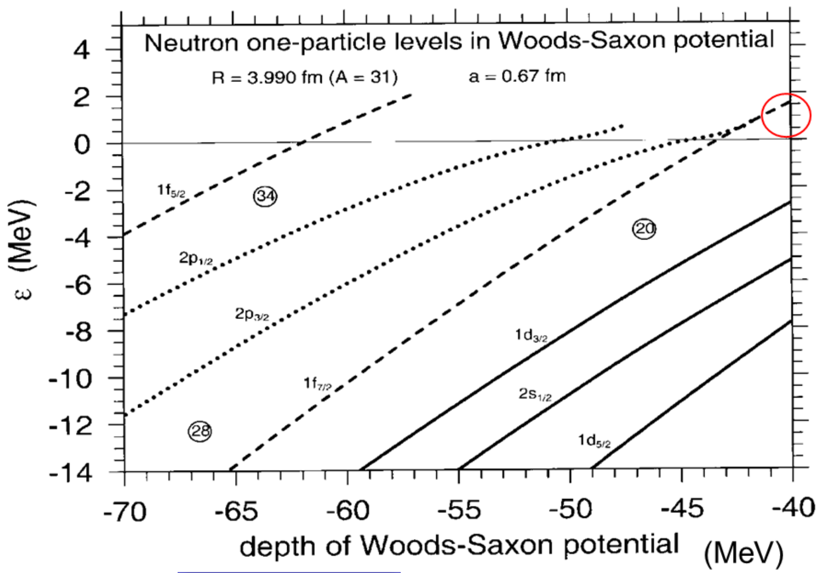

In particular, the trend of s- and p-orbitals becomes almost flat when their energies approach zero.

We expect changes in the shell structure when going far from the stability valley

KS/DFT language

Shell-model language

Mean field

$$U_q(\vec{r}) = \int d^3r' \sum_{q'} v_{qq'}(\vec{r}, \vec{r}\,')\rho_{q'}(r\,')$$

Monopole interaction

$$\hat{v}^m_{nn}(j,j') = \begin{cases} V^m_{nn}(j,j)\,\frac{1}{2}\,\hat{n}_j\,(\hat{n}_j - 1) & \text{for } j = j' \\ V^m_{nn}(j,j')\,\hat{n}_j\,\hat{n}_{j'} & \text{for } j \neq j' \end{cases}$$

Tensor force is a further element that (a) affects the evolution of shell structure and (b) is in common between KS/DFT and SM.

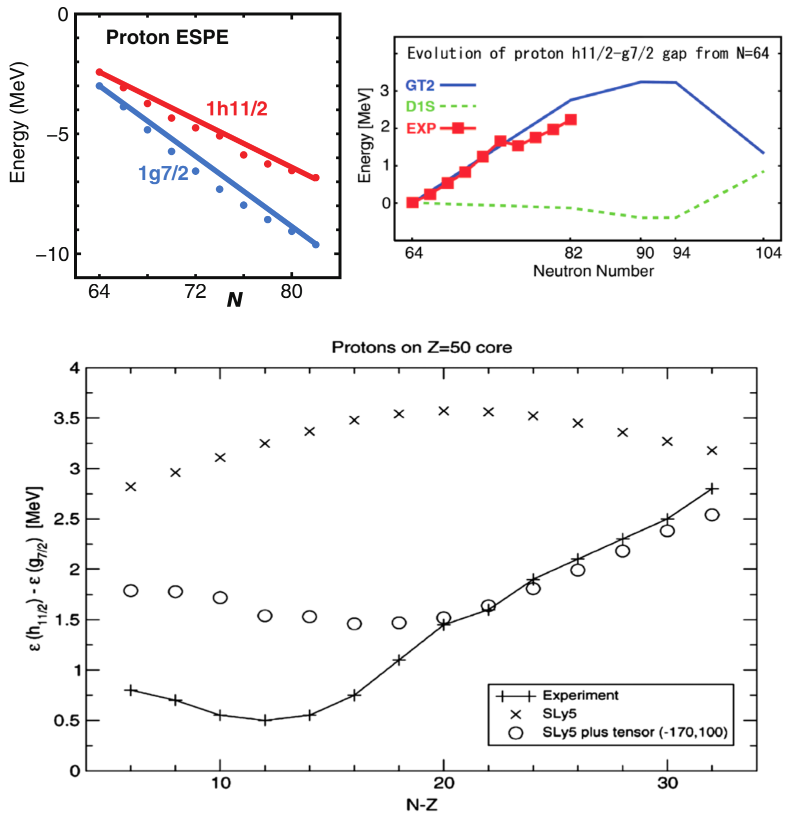

FIG. 32. Evolution of the proton $h_{11/2}$-$g_{7/2}$ gap in the Sb isotopes with and without the tensor term. (Upper left panel) $\pi + \rho$ meson-exchange tensor force on top of the usual Woods-Saxon potential. From Otsuka *et al.*, 2005. (Upper right panel) A Gogny-type calculation with the tensor force (GT2) and without it (D1S). From Otsuka, Matsuo, and Abe, 2006. (Lower panel) A zero-range tensor force calculation added to the SLy5 force. From Colò *et al.*, 2007.

Bonus: neutron stars

The existence of a netron star can be, at our level, understood by means of a simple exercise based on the semi-empirical mass formula,

$$\mathrm{BE}(A,Z) = a_{\mathrm{V}}A - a_{\mathrm{S}}A^{2/3} - a_{\mathrm{A}}\frac{(N-Z)^2}{A} + \text{pairing term.}$$

A system with only neutrons has no Coulomb, and is expected to be very large if the binding energy of the latter formula, which is negative, must be counterbalanced by the gravitational energy (9.7), that we can take with $k = 3/5$ assumung that the density is uniform. Being the system very large, we can neglect the surface energy and obviously the pairing contribution. We arrive at the following balance between nuclear and gravitational energies, namely

$$a_{\mathrm{V}}A - a_{\mathrm{A}}A + \frac{3}{5}\frac{Gm^2}{r_0}A^{5/3} = 0, \tag{9.26}$$

where m is the nucleon mass and the radius is taken as usual from Eq. (2.1).

If we replace reasonable values for the parameters of the mass formula, like $a_{\mathrm{V}} = 15.85$ MeV and $a_{\mathrm{A}} = 23.21$ MeV, we obtain

$$A \approx 5\ 10^{55}. \tag{9.27}$$

The corresponding mass and radius are

$$M = mA \approx 10^{29}\ \mathrm{kg} \approx 0.05\ M_{\odot} \qquad R = r_0 A^{1/3} \approx 5\ \mathrm{km}. \tag{9.28}$$

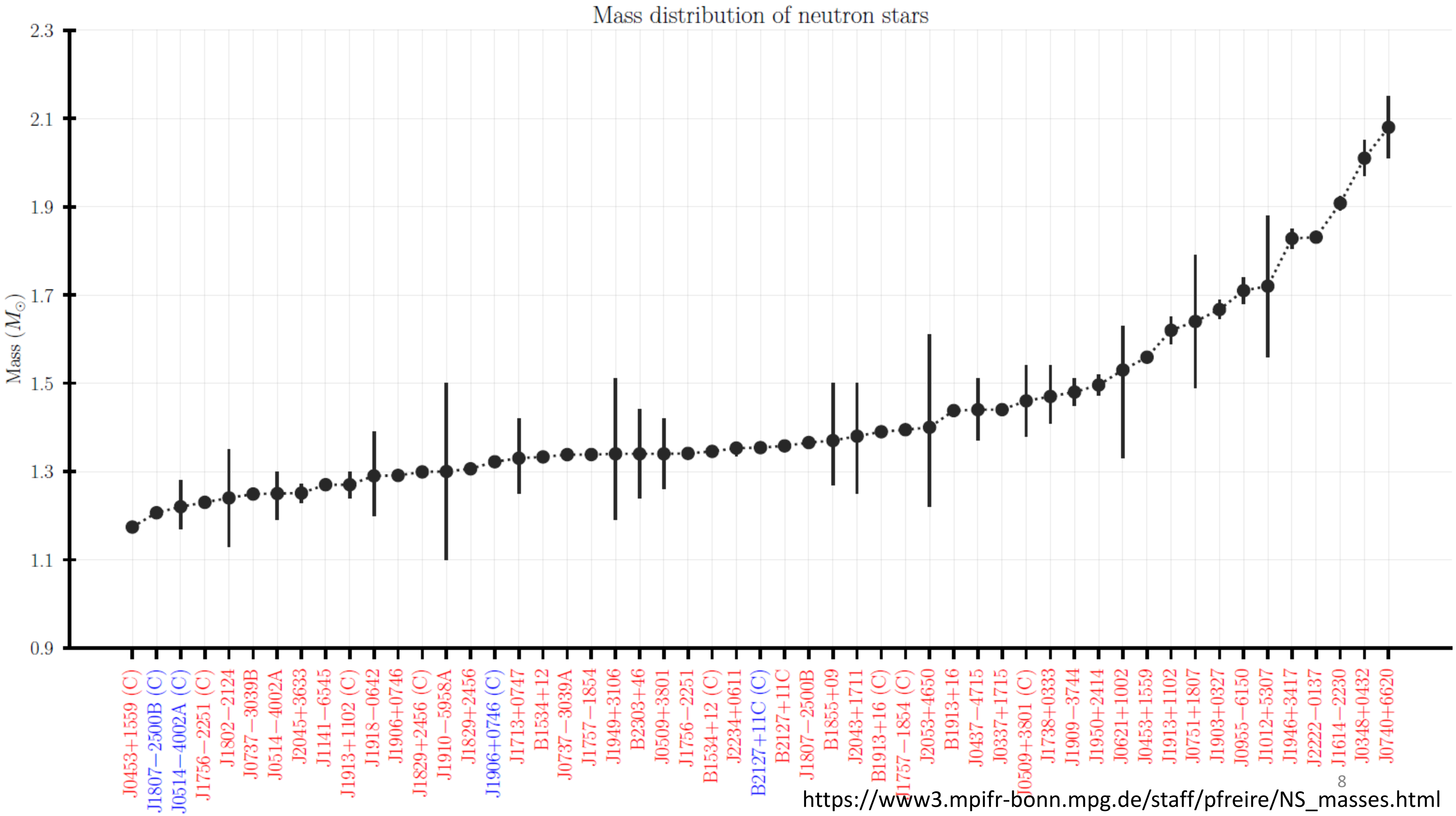

https://www3.mpifr-bonn.mpg.de/staff/pfreire/NS_masses.html

Credit: B. Giacomazzo

Measurements of masses and radii

Up to some time ago, measurements of radii have been plagued by large uncertainties.

Moreover, radii and masses were determined for different systems.

Recently, NASA's NICER mission has measured, for the first time, mass and radius of the same star.

The results will be shown here below.

The observation of gravitational waves has also set new constraints ("chirp mass", see below).

The TOV equation

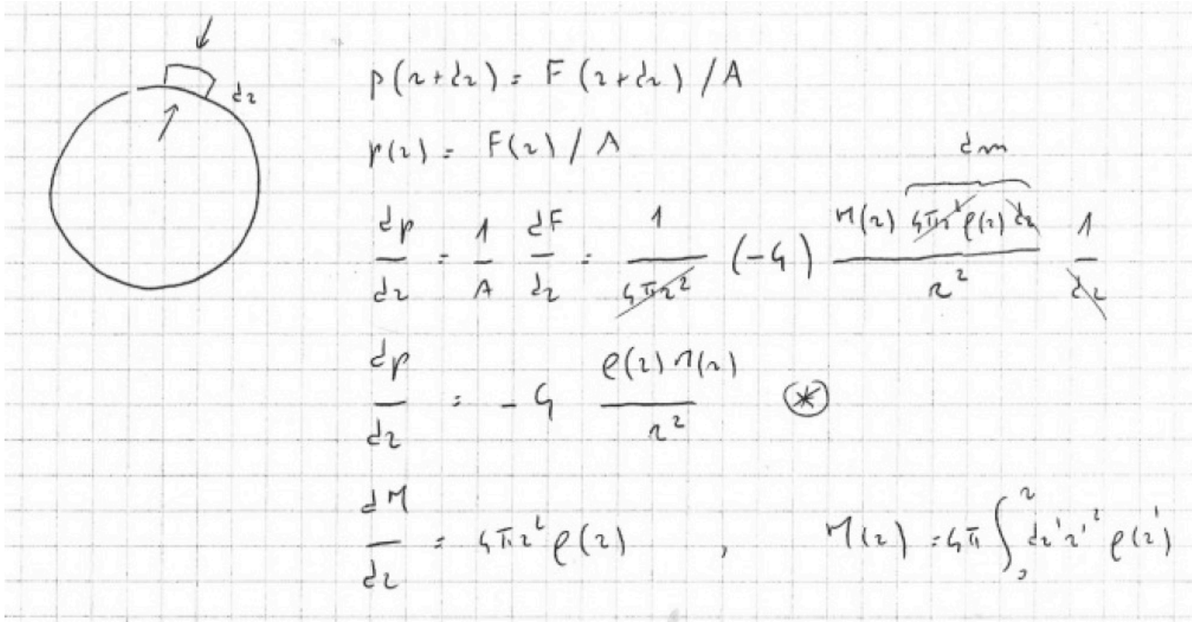

Classical gravity (Newton)

$$\frac{dP(r)}{dr} = -\frac{Gm(r)\varepsilon(r)}{r^2c^2}$$

General relativity corrections (TOV)

$$\frac{dP(r)}{dr} = -\frac{Gm(r)\varepsilon(r)}{r^2c^2}\frac{\left(1+\frac{P(r)}{\varepsilon(r)}\right)\left(1+\frac{4\pi r^3P(r)}{\varepsilon(r)}\right)}{1-\frac{2Gm(r)}{rc^2}}$$

In either case, only

$$P(\rho)$$

is needed

EoS and the solution of the TOV equation

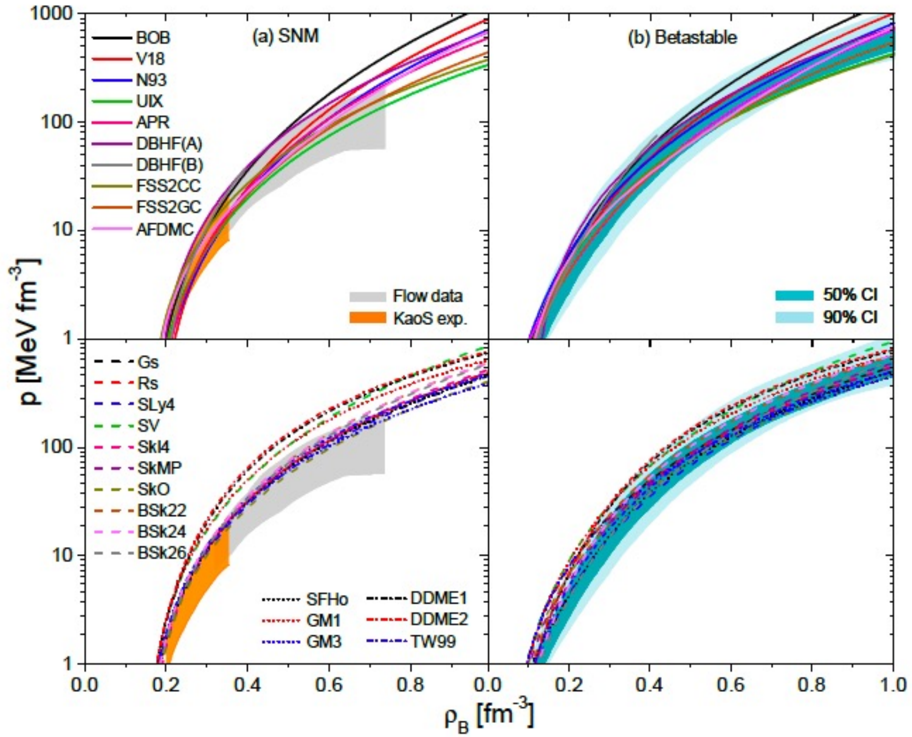

Figure 3. Pressure vs. baryon density for the symmetric case (**left panels**), and the beta-stable case (**right panels**). The upper (lower) panels display results for microscopic (phenomenological) EOSs. Constraints derived from HIC data are displayed in the left panels as orange (KaoS experiment) and grey (flow data) bands. Limits deduced by the GW170817 event are labelled by blue bands in the right panels. See text for details.

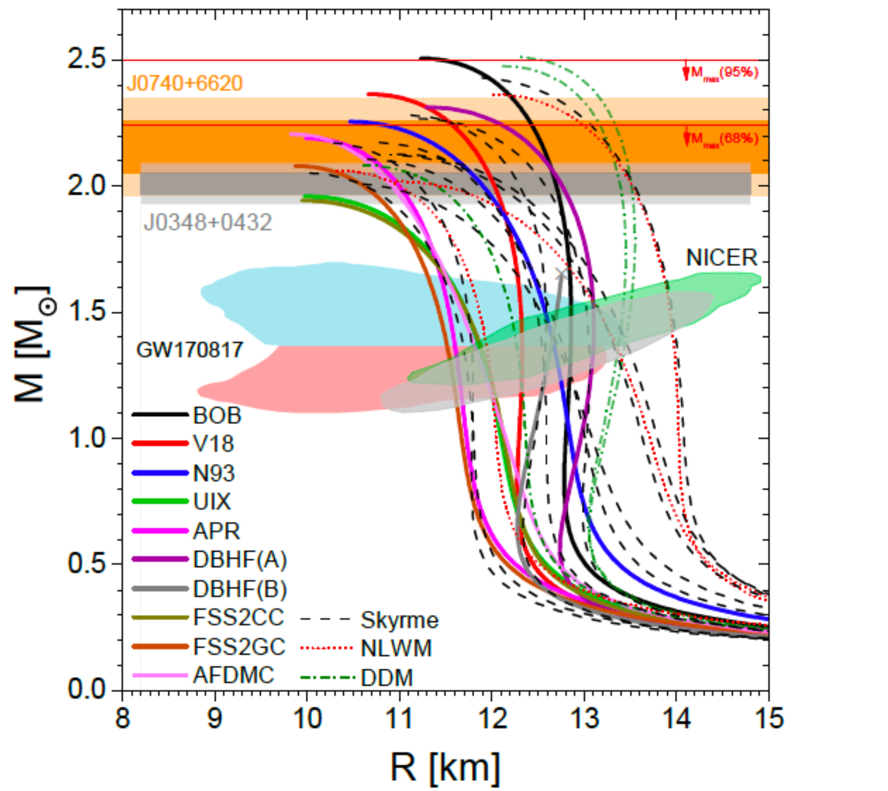

Figure 4. Mass-radius relations predicted by the different EOSs listed in Table 1. The observed masses of the millisecond pulsar PSR J0740 + 6620 [12] and of J0384-0432 [11] are also shown, as well as constraints inferred from the analysis of the GW170817 event and observations reported by the NICER mission [18,19]. See text for details.

F. Burgio *et al*., Symmetry 13, 400 (2021)

Merging of neutron star AND the nuclear EoS

- 2015: first observation of Gravitational Waves (GW), awarded with Nobel prize in 2017.
- 17/8/2017 "multi-messenger" observation of NS merging (GW, GRB, X-rays...).

GW170817 Press Release

LIGO and Virgo make first detection of gravitational waves produced by colliding neutron stars

B.P. Abbott et al., Astrophysical J. Lett. 848:L12 (2017)

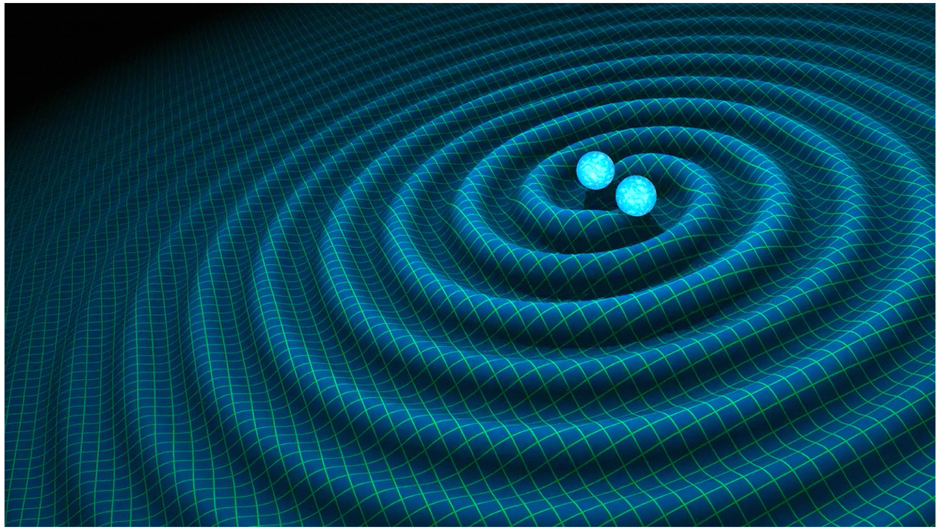

In simulations tidal effects are relevant. A more compact star is harder to distort. But this depends on S!

$$\Lambda = \frac{2}{3} k_2 \left(\frac{c^2 R}{GM} \right)^2$$

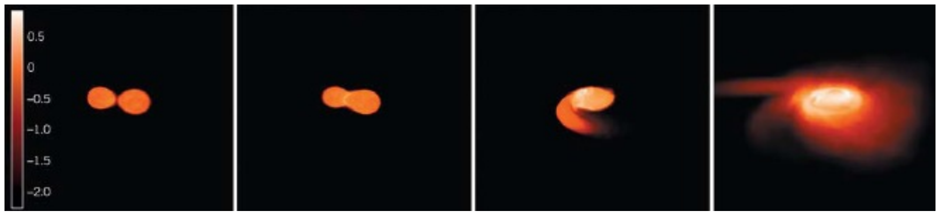

Mass polarizability: ratio quadrupole moment / gravitational field

The Astrophysical Journal Letters, 848:L12 (59pp), 2017 October 20 https://doi.org/10.3847/2041-8213/aa91c9

Multi-messenger Observations of a Binary Neutron Star Merger*

LIGO Scientific Collaboration and Virgo Collaboration, Fermi GBM, INTEGRAL, IceCube Collaboration, AstroSat Cadmium Zinc Telluride Imager Team, IPN Collaboration, The Insight-HXMT Collaboration, ANTARES Collaboration, The Swift Collaboration, AGILE Team, The 1M2H Team, The Dark Energy Camera GW-EM Collaboration and the DES Collaboration, The DLT40 Collaboration, GRAWITA: GRAvitational Wave Inaf TeAm, The Fermi Large Area Telescope Collaboration, ATCA: Australia Telescope Compact Array, ASKAP: Australian SKA Pathfinder, Las Cumbres Observatory Group, OzGrav, DWF (Deeper, Wider, Faster Program), AST3, and CAASTRO Collaborations, The VINROUGE Collaboration, MASTER Collaboration, J-GEM, GROWTH, JAGWAR, Caltech-NRAO, TTU-NRAO, and NuSTAR Collaborations, Pan-STARRS, The MAXI Team, TZAC Consortium, KU Collaboration, Nordic Optical Telescope, ePESSTO, GROND, Texas Tech University, SALT Group, TOROS: Transient Robotic Observatory of the South Collaboration, The BOOTES Collaboration, MWA: Murchison Widefield Array, The CALET Collaboration, IKI-GW Follow-up Collaboration, H.E.S.S. Collaboration, LOFAR Collaboration, LWA: Long Wavelength Array, HAWC Collaboration, The Pierre Auger Collaboration, ALMA Collaboration, Euro VLBI Team, Pi of the Sky Collaboration, The Chandra Team at McGill University, DFN: Desert Fireball Network, ATLAS, High Time Resolution Universe Survey, RIMAS and RATIR, and SKA South Africa/MeerKAT
(See the end matter for the full list of authors.)

Received 2017 October 3; revised 2017 October 6; accepted 2017 October 6; published 2017 October 16

Abstract

On 2017 August 17 a binary neutron star coalescence candidate (later designated GW170817) with merger time 12:41:04 UTC was observed through gravitational waves by the Advanced LIGO and Advanced Virgo detectors. The *Fermi* Gamma-ray Burst Monitor independently detected a gamma-ray burst (GRB 170817A) with a time delay of ~1.7 s with respect to the merger time. From the gravitational-wave signal, the source was initially localized to a sky region of 31 deg^2 at a luminosity distance of 40^{+8}_{-8} Mpc and with component masses consistent with neutron stars. The component masses were later measured to be in the range 0.86 to 2.26 $M_\odot$. An extensive observing campaign was launched across the electromagnetic spectrum leading to the discovery of a bright optical transient (SSS17a, now with the IAU identification of AT 2017gfo) in NGC 4993 (at ~40 Mpc) less than 11 hours after the merger by the One-Meter, Two Hemisphere (1M2H) team using the 1 m Swope Telescope. The optical transient was independently detected by multiple teams within an hour. Subsequent observations targeted the object and its environment. Early ultraviolet observations revealed a blue transient that faded within 48 hours. Optical and infrared observations showed a redward evolution over ~10 days. Following early non-detections, X-ray and radio emission were discovered at the transient's position ~9 and ~16 days, respectively, after the merger. Both the X-ray and radio emission likely arise from a physical process that is distinct from the one that generates the UV/optical/near-infrared emission. No ultra-high-energy gamma-rays and no neutrino candidates consistent with the source were found in follow-up searches. These observations support the hypothesis that GW170817 was produced by the merger of two neutron stars in NGC 4993 followed by a short gamma-ray burst (GRB 170817A) and a kilonova/macronova powered by the radioactive decay of *r*-process nuclei synthesized in the ejecta.

Key words: gravitational waves – stars: neutron

Numerical GR simulations are becoming increasingly accurate

GW from NS-NS merging provide information on the EoS

This is a very active domain in which more progress is expected

PHYSICAL REVIEW LETTERS **129**, 032701 (2022)

Probing the Incompressibility of Nuclear Matter at Ultrahigh Density through the Prompt Collapse of Asymmetric Neutron Star Binaries

Albino Perego,[1,2,*] Domenico Logoteta,[3,4] David Radice,[5,6,7] Sebastiano Bernuzzi,[8] Rahul Kashyap,[5,6] Abhishek Das,[5,6] Surendra Padamata,[5,6] and Aviral Prakash[5,6]

Structure of neutron stars

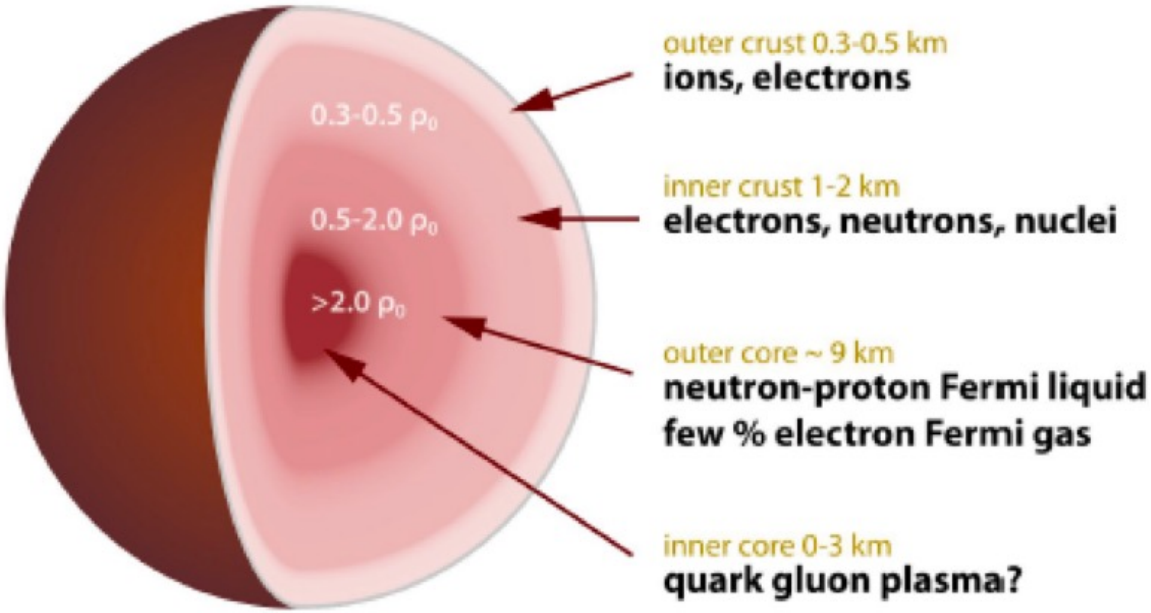

Outer surface of the star: ^{56}Fe atoms.

With increasing density, atoms are ionized and the electrons become relativistic.

Outer crust: nuclei in a lattice, plus electron gas. Electron capture: nuclei become neutron-rich.

Inner crust: nuclei "drip neutrons out”.

Outer core: nuclei and free neutrons coalesce. This defines the so-called outer core. Elongated shapes vs. uniform matter? Balance between surface energy and Coulomb energy.

Inner core: completely uncertain is the composition of neutron stars at even higher densities. Leptons, Σ, Λ, Ξ hyperons? Quark matter??